Preprint
UCRL-JC-136877

Numerical Integration of Elastoviscoplasticity Model with Stiff Hardening and Softening

O.Y. Vorobiev, I.N. Lomov, L.A. Glenn and M.B. Rubin

This article was submitted to
International Conference on Computational Engineering Science,
Los Angeles, CA, August 21-25, 2000

February 1, 2000

U.S. Department of Energy
Lawrence
Livermore
National
Laboratory

ICES2K Conference, August 2000, Los Angeles, USA

Numerical Integration of Elastoviscoplasticity model with Stiff Hardening And Softening.

O.Yu Vorobiev, I.N Lomov, L.A Glenn
Geophysics and Global Security Division
LLNL, CA 94550
M.B Rubin
Faculty of Mechanical Engineering, Technion-Israel Institute of Technology,
32000 Haifa, Israel

P.O Box 808, L-206, LLNL, CA 94550
e-mail: oleg@s90.es.llnl.gov

Summary

The constitutive equations for viscoplasticity typically are stiff differential equations and require special numerical methods to intergrate them efficiently. The objective of this paper is to propose a class of rate-dependent viscoplastic constitutive equations which can be integrated by an efficient explicit scheme that includes the first order effect of pressure and plastic strain hardening.

INTRODUCTION

The strength of many geological materials and some metals exhibits a high sensitivity to the plastic strain and the pressure. To produce stable results for these materials using the constitutive equations for viscoplasticity may require implicit integration . We propose a class of rate-dependent viscoplastic constitutive equations which can be integrated by an efficient explicit scheme that includes the first order effect of hardening. To model the dynamic response of material, the system of equations representing the mass, momentum and energy conservation laws is supplemented by the following equation for the unimodular tensor of elastic distortional deformation **B** [1].

$$\dot{\mathbf{B}} = \mathbf{L}\mathbf{B} + \mathbf{B}\mathbf{L}^{T} - \frac{2}{3}(\mathbf{D}\bullet\mathbf{I})\mathbf{B} - \Gamma_{p}\left[\mathbf{B} - \frac{3\mathbf{I}}{\mathbf{B}^{-1}\bullet\mathbf{I}}\right] \quad (1)$$

Using **B,** the deviatoric stress $\mathbf{T}'$ can be expressed as $\mathbf{T}' = G\,\frac{\rho(1-\Phi)}{\rho_0}(\mathbf{B} - \frac{1}{3}(\mathbf{B}\bullet\mathbf{I}))$, where G is the shear modulus, ρ_0 and ρ are the initial and the current density and Φ is the reference porosity. In (1), Γ_p specifies the plastic response of the material and is taken to be a function of the von Mises effective stress σ_e and the yield strength Y proposed in [2]:

$$\Gamma_p = \Gamma_{p0}\left(\frac{3G}{\sigma_e}\right)\left(\frac{\langle\sigma_e - Y\rangle}{Y_0}\right)^2 \quad (2)$$

In the test problems considered the conservation laws were integrated numerically using the second order Godunov scheme. More details about the numerical algorithm can be found in [3].
We focus our attention on integration of Eq.(1) in the case of a general strength model, which includes a set of softening and hardening effects attributed to different physical phenomena such as bulking, distortional damage, porosity compaction, tensile failure. We study possible instabilities cased by these effects in numerical simulation and formulate constrains on the model parameters to avoid these instabilities.

STRENGTH OF MATERIAL

The physical phenomena that influence the yield strength **Y** are taken into account using a multiplicative form with **Y** given by:

$$Y = Y_0 F_1(\xi, p) F_2(p) F_3(\Omega, p) F_4(\beta, p) F_5(\rho, \varepsilon) \qquad (3)$$

The first two terms in (3) describe hardening and the last three describe softening effects.

F_1 is specified in terms of hardening parameters ξ by the form $F_1 = 1 + (k_1 - 1)\xi$, where the value of k_1 gives the maximum strain hardening when $\xi = 1$. The hardening parameter ξ is determined by an evolution equation of the form

$$\dot{\xi} = k_2 \left[\frac{\dot{\varepsilon}_p}{F_2(p)} \right] (1 - \xi) \qquad (4)$$

The pressure hardening F_2 is typical for rock materials and is due to increased friction between the grains at compression.

The damage function F_3 specified by (6) makes material weak at low pressures $p \le p_0$ once it is damaged.

$$F_3 = 1 - k_5 \Omega \exp\left[-\frac{\langle p \rangle}{p_0} \right] \qquad (5)$$

The damage parameter, Ω, used in the function (5) is evaluated using the relation

$$\dot{\Omega} = \frac{\langle T_{\max} - T_{th} \rangle}{\tau_{dam} Y_0} \quad \text{if } \xi = 1 \qquad (6)$$

where $T_{\max}$ is the most compressive principal stress, T_{th} is the threshold stress for damage growth, and τ_{dam} is a characteristic time for damage. The damage begins to accumulate when the hardening parameter ξ is equal to unity. F_4 is a function of the Lode angle and F_5 models the effect of melting at high pressures.

BULKING MODEL

Strong distortional deformations can cause microfracturing that tends to increase porosity in rock materials. This leads to the build up of the pressure since more volume is occupied by microcracks. The high pressure, in turn, affects the yield through the hardening term F_2.

The evolution of porosity due to bulking is chosen to be proportional to the rate of plastic dissipation and is given by Eq.(8) below.

$$\dot{\phi} = (1-\phi)\frac{m_d \dot{\varepsilon}_p \sigma_e \langle \phi^* - \phi \rangle}{Max(p^*, p)} \qquad (8)$$

The value of ϕ^* specifies the maximum bulking porosity that can be achieved and the function m_d determines the rate of bulking. The plastic strain rate can be expressed in terms of $\mathbf{B}$ as

$$\dot{\varepsilon}_p = \frac{\Gamma_p}{2}\sqrt{\tfrac{2}{3}}\mathbf{B}' \bullet \mathbf{B}' \qquad (9)$$

THE SCHEME OF INTEGRATION AND TEST RESULTS

We have modified the scheme of integration of the Eq.(1) developed in [1] accounting for the plastic strain and the pressure dependence of the yield strength. According to [1] Eq.(1) first solved without plasticity term to find elastic trial value of $\mathbf{B}^*$ and corresponding von Mises stress σ_e^*. Then to satisfy (1) the new values of $\mathbf{B}$ can be found as $\mathbf{B} = \lambda \mathbf{B}^*$, where λ is a scale factor given by (10)

$$1 - \lambda = \Delta t \Gamma_p \lambda \qquad (10)$$

The value of Γ_p in (10) is taken at the end of the time step.
Substituting (2) into (10) we have (11)

$$\lambda + \frac{3\Gamma_{p0} G}{Y_0^2 \sigma_e^*}(\sigma_e^* \lambda - Y)^2 = 1 \qquad (11)$$

The yield strength at the end of the time step used in (11) can be written using serial expansion as

$$Y = Y^* + \left(\frac{\partial Y}{\partial \varepsilon_p}\right)\Delta\varepsilon_p + \left(\frac{\partial Y}{\partial p}\right)\Delta p \qquad (12)$$

The increment of the plastic strain during the time step can be expressed in terms of λ using (9) and (10) as

$$\Delta\varepsilon_p = (1-\lambda)\frac{\sigma_e^*}{3G} \qquad (13)$$

The change in the pressure is due to generation of bulking porosity. According to (8) it is roughly proportional to the change in plastic strain as

$$\Delta p \approx K\Delta\varphi = \frac{(1-\varphi)Km_d\langle\varphi^* - \varphi\rangle\sigma_e}{p}\Delta\varepsilon_p \quad (14)$$

So (12) can be written as $Y = Y^* + A(1-\lambda)$ (15)

where A can be found from (12)-(14). Thus (11) transforms into (16)

$$\lambda + \frac{3\Gamma_{p0}G}{Y_0^2\sigma_e^*}((\sigma_e^* + A)\lambda - (Y^* + A))^2 = 1 \quad (16)$$

Solving (16) for λ we have

$$\lambda = \begin{cases} 1 & for\ \sigma_e^* < Y^* \\ \dfrac{\bar{\lambda}Y_o + Y^* + A}{\sigma_e^* + A} & for\ \sigma_e^* \geq Y^* \end{cases} \quad (17)$$

where $\bar{\lambda} = \dfrac{-d_1 + \sqrt{d_1^2 - 4d_2d_0}}{2d_2}$ and $d_0 = \dfrac{Y^* + A}{\sigma_e^* + A} - 1;\ d_1 = \dfrac{Y_0}{\sigma_e^* + A};\ d_2 = \dfrac{(\Delta t\Gamma_{po})3G}{\sigma_e^*}$

If $\Gamma_{po} \to \infty$ we get a rate-independent case , where λ can be found as

$$\lambda = \begin{cases} 1 & for\ \sigma_e^* < Y^* \\ \dfrac{Y^* + A}{\sigma_e^* + A} & for\ \sigma_e^* \geq Y^* \end{cases} \quad (18)$$

Parameter λ in (18) gives well known scale factor used in radial return method when $A \to 0$.

The test results shown below illustrate the behavior of granite in uniaxial strain loading. For granite the model described above has been used with the initial yield Y_0=0.02 GPa. Due to the plastic strain hardening the yield strength could increase in a factor of 2.

It is seen from fig.1-2 that introducing correction for plastic strain hardening when calculating the plastic strain makes a big effect. For rate dependent model this effect is not so big at high deformation rates (for example in Fig.3 in rate dependent case both curves with and without correction coincide) but still significant at low deformation rates taking place in big scale events (see Fig.4).

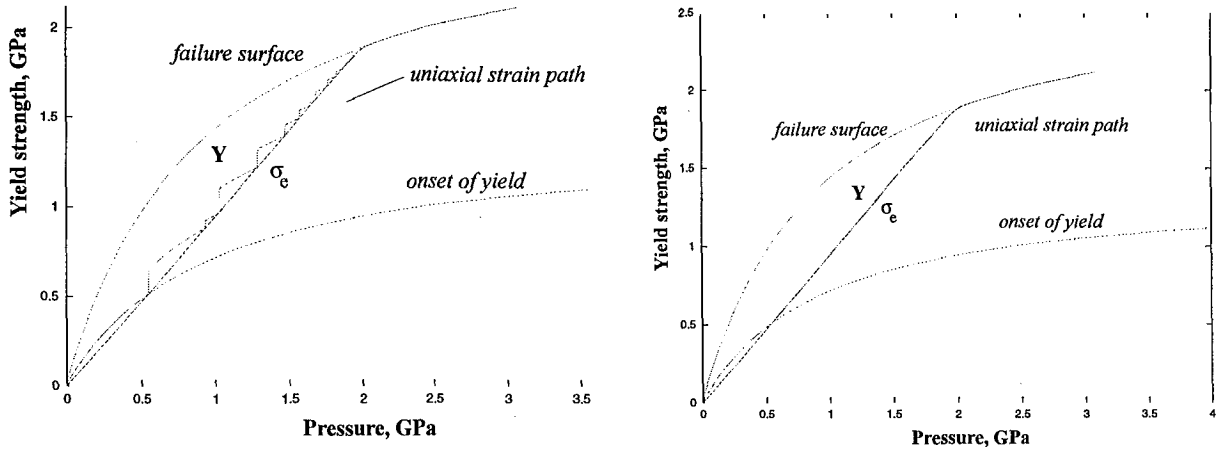

a) b)

Fig.1 Evolution of von Mises stress and the yield strength in uniaxial strain loading for the Granite. Rate independent model without (a) and with (b) correction for plastic strain hardening is used.

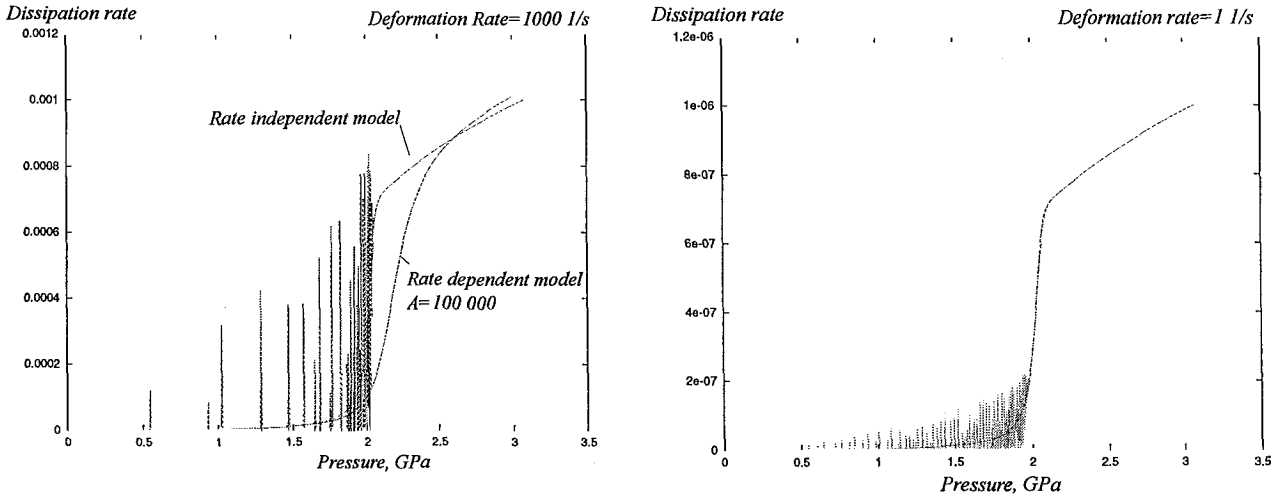

a) b)

Fig.2 Evolution of the dissipation rate $\dot{\varepsilon}_p \sigma_e$ in uniaxial strain loading for rate dependent model with and without correction for plastic strain hardening. The rate of deformation is: a)1000 (1/s), b) 1. (1/s).

1D IMPACT SIMULATION

The difference in results obtained with and without correction on plastic strain hardening is noticeable already in 1D plane problems. The Fig.3 show the results of Granite on Granite impact. It is seen that the shock wave propagates with different velocities in these two cases